An Extension of BSIM3 Model Incorporating Velocity Overshoot

Dennis Sinitsky, Fariborz Assaderaghi, Michael Orshansky, Jeffrey Bokor, and Chenming Hu*

Department of EECS, University of California, Berkeley, CA, 94720; * IBM Corp., East Fishkill, NY

Abstract

In this paper velocity overshoot in Si inversion layers is studied. A simple analytical MOS current drive model that takes velocity overshoot into account is deduced and verified with an energy transport simulator as well as experimental data. The formula for I_d looks very much like the conventional BSIM3 expression. Device scaling based on the model is studied. A new mechanism of MOSFET output conductance due to velocity overshoot is identified.

Introduction

As MOSFET channel length shrinks below 0.25 μm, conventional physical drift-diffusion models are unable to correctly predict I_{dsat} because of electron velocity overshoot. Velocity overshoot was experimentally observed in short-channel devices in [1-3]. Recently, several MOSFET analytical models have been proposed [4-7]. Our approach emphasizes carrier temperature dependence of hot-carrier scattering and nonlocal carrier temperature relaxation, and yields a formula for I_d very similar to a conventional BSIM3 expression.

Derivation of the model

Fig. 1 illustrates the concept of nonlocal temperature relaxation. Assuming an abrupt step electric field profile, temperature T_e of a carrier in such a field is not abruptly changing, but it is relaxing to the high-field steady state value with a characteristic time constant $\tau_e \approx 0.3$ ps roughly independent of T_e [9]. In other words, T_e is lower for higher gradients of E, but for low gradients of E there is a one-to-one correspondence between T_e and the value of E. That is why the relation $\mu=\mu(E)$ is valid only for small gradients of E. For arbitrary field profiles, carrier mobility depends on carrier energy $\varepsilon = \frac{3}{2}kT_e + \frac{m_e v_{drift}^2}{2}$ [10]. In the high field region v_{drift} is a slowly varying quantity, and we can simply assume $\mu=\mu(T_e)$.

We start by writing the expression for T_e in the channel [8]:

$$qnEv - \frac{d}{dx}\left(5nkT_e v/2\right) - \frac{3nk\left(T_e - T_o\right)}{2\tau_e} = 0$$

Here n is electron concentration, E is tangential electric field, v is the electron velocity, T_o is the lattice temperature. For mobility the following expression is used :

$$v = \mu E = \mu_o \frac{T_o}{T_e} E \qquad for \;\; T_e < T_{sat}$$

$$v = const \qquad for \;\; T_e \geq T_{sat}$$

Note that the pre-saturation mobility model holds well for hot electrons [10], and for T_e low $v \propto T_e^{-1/2}$, but we are making this approximation in order to obtain an analytic solution. Since carrier scattering depends on T_e rather than on E, we introduce the concept of T_{sat} - the carrier temperature at which phonon scattering becomes so high that velocity levels out. In a conventional model, the saturation temperature T_{sat} is reached at a point in the channel where $E=E_{sat}$. Fig. 2 shows how the lower nonlocal temperature together with the T_{sat} concept yield a higher effective E_{sat} and give velocity overshoot. The T_e equation becomes:

$$n\mu_o \frac{T_o}{T_e} E^2 - \frac{d}{dx}\left(5k\mu_o T_o nE/2q\right) - \frac{3nk\left(T_e - T_o\right)}{2\tau_e q} = 0$$

In order to solve for T_e, approximate $E=E_m x/L$ in the pre-saturation region. Since from current continuity $nv=const$, and in the region close to velocity saturation v changes slowly, we neglect $E\nabla n$ term as compared to $n\nabla E$. Then expression for T_e becomes:

$$-\mu_o T_o E^2 + \frac{5kT_o\mu_o}{2q}\frac{dE}{dx}T_e + \frac{3k}{2\tau_e q}\left(T_e - T_o\right)T_e = 0$$

The local solution is obtained by dropping the derivative term:

$$T_e^{local} = \frac{1}{2}\left[T_o + \sqrt{T_o^2 + \frac{8}{3}\frac{q\tau_e E^2 \mu_o T_o}{k}}\right] \approx \sqrt{\frac{2}{3}\frac{q\tau_e E^2 \mu_o T_o}{k}}$$

We treat the nonlocal term as a perturbation: $T_e=T_e^{local}+\delta T_e$, and obtain the expression for T_{sat}:

$$T_{sat} = \frac{1}{2}\left[T_o + \sqrt{\frac{8q\tau_e\mu_o T_o}{3k}} E_{sat}^{nonloc}\right] - \frac{5}{6}\tau_e\mu_o\frac{dE}{dx}T_o = \frac{1}{2}\left[T_o + \sqrt{\frac{8q\tau_e\mu_o T_o}{3k}} E_{sat}^{loc}\right]$$

This allows to directly relate E_{sat}^{loc} and nonlocal E_{sat} in both triode and saturation regions:

$$E_{sat}^{triode} = E_{sat}^{loc} + \sqrt{\frac{25\tau_e^{\ 2}\mu_o^2 T_o^2 \cdot 3k}{36 \cdot 8q\tau\mu_o T_o}\frac{V_d}{2L^2}} \approx E_{sat}^{loc} + 0.255\sqrt{\frac{\tau_e \mu_o T_o k}{q}\frac{V_d}{L^2}}$$

$$E_{sat}^{saturation} \approx E_{sat}^{loc} + 0.255\sqrt{\frac{\tau_e \mu_o T_o k}{q}\frac{V_d}{(L-\Delta L)^2}}$$

This is the saturation field we now use in the conventional BSIM3 formula for I_d:

$$I_d^{triode} = \frac{W}{L}\mu_o C_{ox}\left(V_g - V_t - \frac{V_d}{2}\right)\cdot V_d \frac{1}{1+(V_d / E_{sat}L)}$$

$$I_d^{saturaton} = \frac{1}{2}WC_{ox}\mu_o E_{sat}\frac{(V_g - V_t)^2}{\left[V_g - V_t + E_{sat}(L-\Delta L)\right]}$$

Here ΔL is channel length shortening due to channel length modulation [11]. Note that E_{sat} has also ΔL dependence buried in it. This is an additional mechanism for reduction of R_{out}. The meaning of it is that as V_d increases, the gradient of electric field increases as well, but not only because of direct V_d increase, but also channel length modulation, and that gives rise to even more velocity overshoot.

The fits for TMA-MEDICI simulated MOSFETs with various L_{eff} are shown in Fig. 1 a-d. Note that all four devices have the same x_j and t_{ox}, so all four fits use the same set of fitting parameters. First, conventional BSIM3 formula was used to fit drift-diffusion simulations. Then τ_e was fitted to energy-balance simulation data. Fitting to a 0.1 μm experimental data is shown in Fig. 2. DIBL parameters were extracted from parallel shift of $log(I_d)$-V_g subthreshold curves. Current levels and output conductance clearly show presence of velocity overshoot in a device. The plot of I_{dsat} vs. L_{eff} in Fig. 3 emphasizes this point.

Impact of velocity overshoot on scaling

To study the impact of velocity overshoot on scaling, we employ five different technologies presented in Table 1. Fig. 4 shows the projected effect of velocity overshoot on I_{dsat}. The sharp drops in I_{dsat} are due to drop in V_{dd} when we go from one technology family to another. Although overshoot has no impact for devices with L_{eff} above .3 μm, it starts to play an important role in the sub-.3 μm regime, and increases faster than exponentially in L_{eff}.

The series resistance tends to minimize the effect of velocity overshoot because more current drops more voltage on R_s effectively reducing the V_{gs}, as shown in Fig. 5. The effect is stronger for shorter channel length.

Finally, the effect of velocity overshoot on V_{dsat} is shown in Fig. 6. As L_{eff} shrinks, V_{dsat} becomes higher than predicted by a conventional model because it is harder to saturate the device, as evident from Figs. 1,2. The V_{dsat} calculated using conventional and velocity overshoot models are the same for L_{eff}>0.2μm, but differ for shorter channel lengths.

Summary

An analytical model for MOSFET I_d that incorporates velocity overshoot was developed. The formula resembles the conventional BSIM3 formula with a modified saturation field E_{sat}. A good agreement of the model with simulations and experimental data is shown. Influence of velocity overshoot on scaling and device parameters was studied.

Acknowledgments

This work was supported by a grant from Intel Corp., Joint Services Electronics Program, under grant number F49620-94-C-0038, and Air Force Office of Scientific Research, Air Force Materiel Command, USAF, under grant number F49620-94-1-0464. We acknowledge TMA inc. for providing a device simulator MEDICI. Device fabrication was done in the U.C.Berkeley Microlab. Useful discussions with Dr. Clement H. Wann are greatly appreciated.

References

1. G. A. Sai-Halasz *et al*, *IEEE Electron Device Lett.*, vol. **9**, no. 9, p.p. 464-466, September 1988.
2. G. G. Shahidi *et al*, *IEEE Electron Device Lett*, vol. **9**, no. 2, p.p. 94-96, February 1988.
3. F. Assaderaghi *et al*, in *IEDM Tech. Dig.*, p.p. 479-482, 1994.
4. S.-Y. Ma *et al*, *Jpn. J. Appl. Phys.*, Vol. 33, pp 550-553, 1994.
5. K. Sonoda *et al*, *IEEE Trans. Electron Dev.*, Vol. 38, No. 12, p.p. 2662-2668, December 1991.
6. V. K. De *et al*, *IEDM Tech. Dig.*, p.p. 717-720, 1993.
7. J.-H. Song *et al*, *IEEE Trans. Electron Dev.*, p.p. 1870-1875, November 1996.
8. E. Takeda *et al*, *IEEE Trans. Electron Devices*, ED-29, no. 4, p. 611, 1982.
9. G. Baccarani *et al*, *Solid-State Electron.*, vol. **28**, no. 4, pp. 407-416, 1985.
10. M. Lundstrom, "Fundamentals of Carrier Transport", Vol. X of "Modular Series on Solid State Devices", editors G. W. Neudeck, R. F. Pierret, Addison Wesley Co., 1990.
11. Z. Liu *et al*, *IEEE Trans. Electron Dev.*, Vol. 40, No. 1, p.p. 86-94, January 1993.

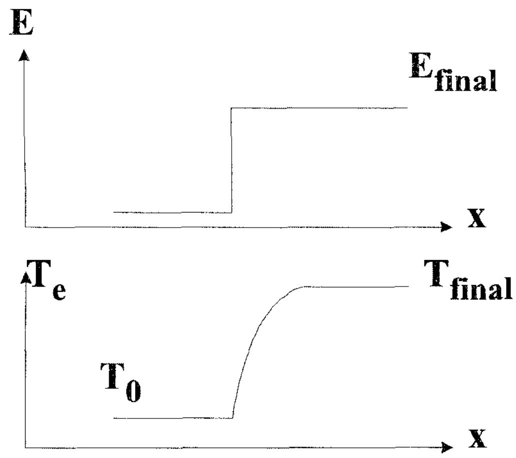

Fig. 1 Illustration of a concept of nonlocal temperature

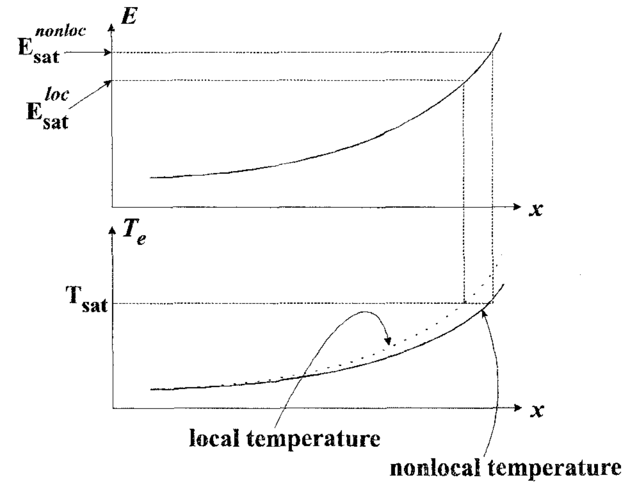

Fig. 2 The concept of T_{sat} yielding a higher E_{sat}

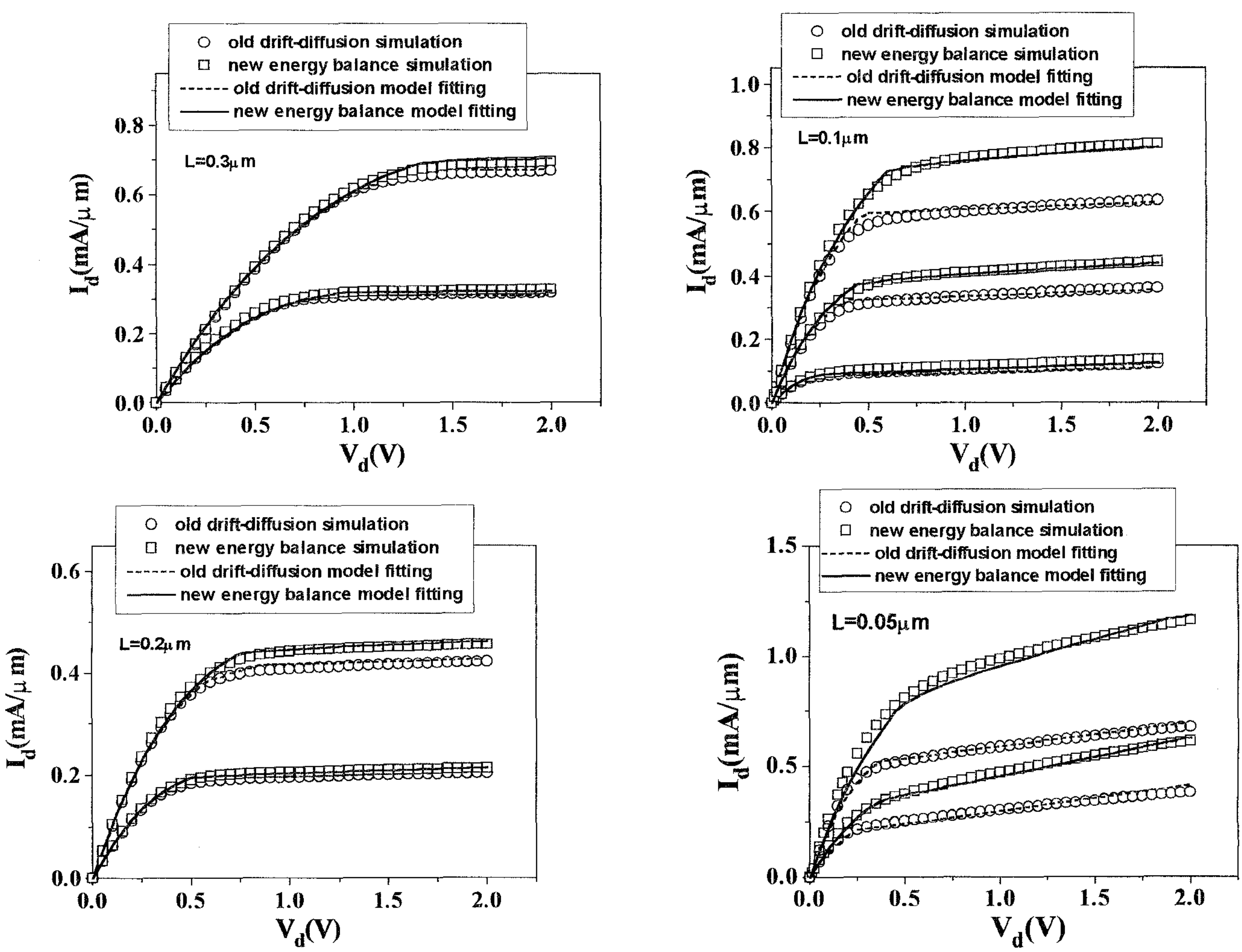

Fig. 3 a-d. The model fit to MEDICI 2-D simulations for different channel lengths.

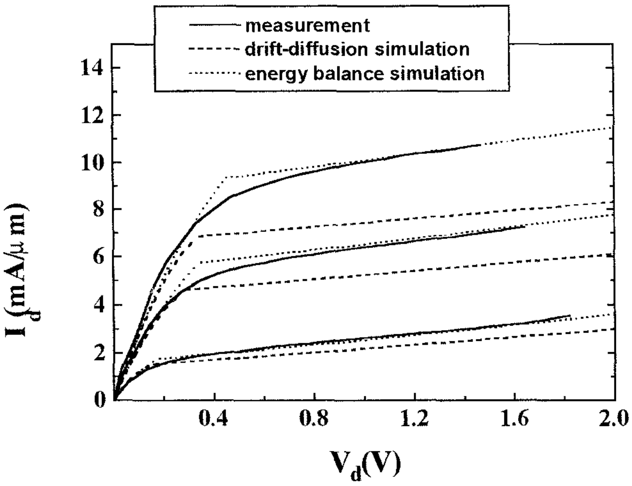

Fig. 4 The model fit to experimental data; L_{eff}=0.1μm.

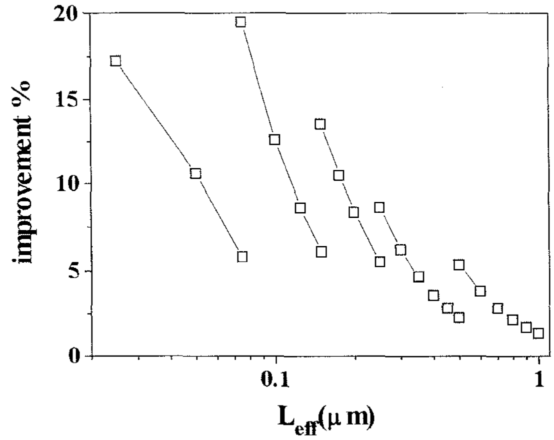

Fig. 6 Current improvement due to overshoot

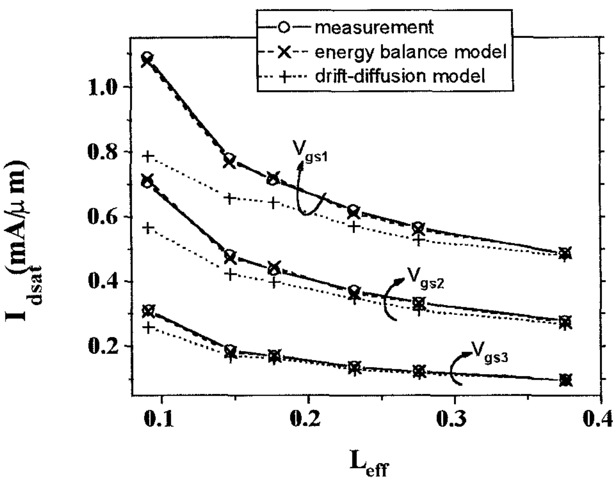

Fig. 5 I_{dsat} vs L_{eff} for three different gate voltages.

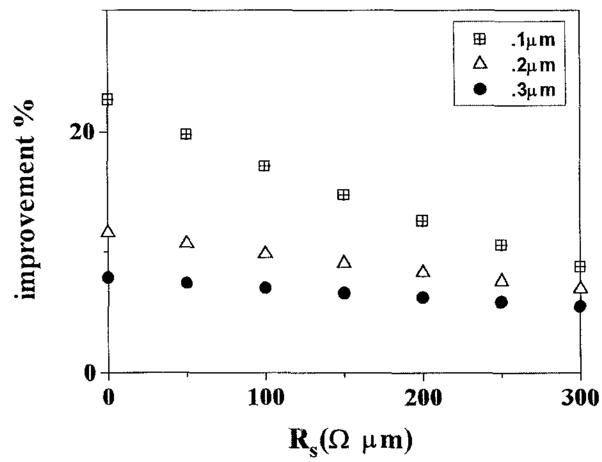

Fig. 7 Current improvement degradation due to R_s

L_{eff}(μm)	T_{ox}(Å)	V_t(V)	V_{dd}(V)
.025-.075	25	.3	1
.075-.15	40	.4	1.5
.15-.25	60	.45	2.5
.25-.5	80	.5	3.3
.5-1	150	.7	5

Table 1. Parameters for a scaling study

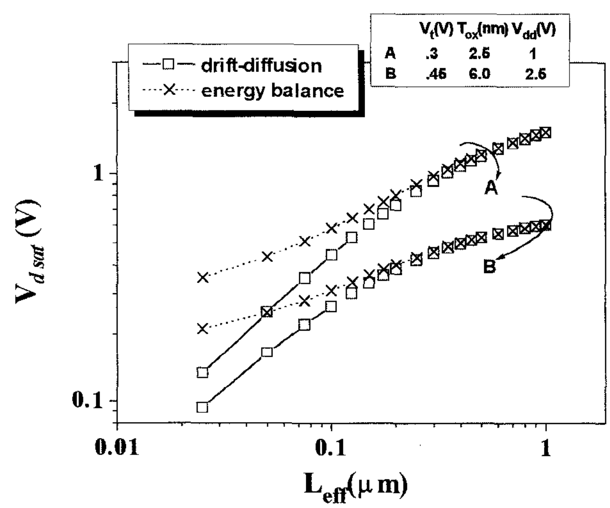

Fig. 8 V_{dsat} scaling for v_{sat} = $8 \cdot 10^6$ cm/sec, drift-diffusion and the velocity overshoot cases.